NEUROSCIENCE

Near-infrared deep brain stimulation via upconversion nanoparticle–mediated optogenetics

Shuo Chen,[1]* Adam Z. Weitemier,[1] Xiao Zeng,[2] Linmeng He,[1] Xiyu Wang,[1] Yanqiu Tao,[1] Arthur J. Y. Huang,[1] Yuki Hashimotodani,[3] Masanobu Kano,[3,4] Hirohide Iwasaki,[5] Laxmi Kumar Parajuli,[5] Shigeo Okabe,[5] Daniel B. Loong Teh,[6] Angelo H. All,[7] Iku Tsutsui-Kimura,[8] Kenji F. Tanaka,[8] Xiaogang Liu,[2,9]* Thomas J. McHugh[1,10]*

Optogenetics has revolutionized the experimental interrogation of neural circuits and holds promise for the treatment of neurological disorders. It is limited, however, because visible light cannot penetrate deep inside brain tissue. Upconversion nanoparticles (UCNPs) absorb tissue-penetrating near-infrared (NIR) light and emit wavelength-specific visible light. Here, we demonstrate that molecularly tailored UCNPs can serve as optogenetic actuators of transcranial NIR light to stimulate deep brain neurons. Transcranial NIR UCNP-mediated optogenetics evoked dopamine release from genetically tagged neurons in the ventral tegmental area, induced brain oscillations through activation of inhibitory neurons in the medial septum, silenced seizure by inhibition of hippocampal excitatory cells, and triggered memory recall. UCNP technology will enable less-invasive optical neuronal activity manipulation with the potential for remote therapy.

Technologies for minimally invasive and remote stimulation of specific neurons deep in the brain have long been desired for the experimental interrogation of neural systems and clinical treatment of neurological disorders. Deep brain stimulation is effective in the alleviation of specific neurological symptoms, but lacks cell-type specificity and requires permanently implanted electrodes (*1*). Potential alternatives for brain tissue–penetrating stimuli include electric (*2*, *3*), magnetic (*2*, *4*, *5*), acoustic (*6*, *7*), and optical signals (*8*). These approaches were largely developed independently of the optogenetic toolbox established over the past decade (*9*) and therefore remain limited to discrete applications. Stimulation of deep brain neurons via light-gated ion channels has hitherto required the insertion of invasive optical fibers because the activating blue-green wavelengths are strongly scattered and absorbed by endogenous chromophores (*10*). The action spectra of red-shifted variants of rhodopsins still fall short of the near-infrared (NIR) optical window (650 to 1350 nm), where light has its maximal depth of penetration (*10*–*15*). Two-photon optogenetic methods allow in vivo stimulation via an NIR laser, but the depth of this focal excitation is restricted to shallow brain areas by light scattering (*16*).

We developed transcranial NIR optogenetic stimulation of specifically labeled neurons in deep brain areas, where tissue-penetrating NIR light is locally converted to visible light at levels sufficient for activating channelrhodopsin-expressing neurons (Fig. 1A). This requires lanthanide-doped upconversion nanoparticles (UCNPs) capable of converting low-energy incident NIR photons into high-energy visible emission with an efficiency orders of magnitude greater than that of multiphoton processes (Fig. 1, B to D) (*17*, *18*). As a result, a continuous-wave (CW) NIR laser diode at low-energy irradiance was sufficient to drive intense upconversion emission by UCNPs. Owing to the ladderlike electronic energy structure of the lanthanide, the emission of UCNPs can be precisely tuned to a particular wavelength by control of energy transfer via selective lanthanide-ion doping (*17*, *18*). Incorporation of Tm^{3+} into Yb^{3+}-doped host lattices leads to blue emission that matches the maximum absorption of channelrhodopsin-2 (ChR2) for neuronal activation, whereas the Yb^{3+}-Er^{3+} couple emits green light compatible with activation of halorhodopsin (NpHR) or archaerhodopsin (Arch) for neuronal inhibition (Fig. 1, C and D, and figs. S1 and S2). UCNP-mediated optogenetics was first proposed in 2011 (*19*) and used for neural stimulation in culture (*20*–*22*) and in *Caenorhabditis elegans* (*23*) and zebrafish larvae (*24*), but its compelling potential for minimally invasive deep brain stimulation in a mammalian system has yet to be demonstrated.

We reasoned that UCNP-mediated optogenetics would be feasible for transcranial stimulation of deep brain neurons in rodents based on an evaluation of (i) the efficiency of NIR upconversion by the nanoparticles (Fig. 1D and fig. S3) and (ii) the transmittance of NIR light in brain tissue (figs. S4 and S5). For ChR2 activation, we synthesized blue-emitting $NaYF_4$ nanocrystals codoped with Yb^{3+}/Tm^{3+} (Fig. 1C). An optically inert shell layer of $NaYF_4$ was epitaxially grown onto the core to eliminate the surface quenching of upconversion luminescence by solvent molecules. The resulting core-shell UCNPs exhibited a characteristic upconversion emission spectrum peaking at 450 and 475 nm upon excitation at 980 nm (Fig. 1D). The conversion yield of NIR to blue light was ~2.5% (Fig. 1D and fig. S3). Applying the Kubelka-Munk theory of light propagation in diffuse scattering media (*25*), we estimated that a 2.0-W 980-nm laser delivered over the mouse skull through an optic fiber (200 μm in diameter) would result in 13.8-mW/mm^2 NIR at a depth of 4.5 mm in the brain. At this intensity, local upconversion by UCNPs would generate 0.34-mW/mm^2 blue-light emission (supplementary text), sufficient to activate ChR2 for cation influx (fig. S6).

We therefore performed in vivo fiber photometry (*26*) to examine NIR upconversion by UCNPs in the ventral tegmental area (VTA) of the mouse brain, a region located ~4.2 mm below the skull. UCNPs were injected into the VTA, and an optic fiber was positioned nearby to record blue emission (Fig. 1, F and G). Upon transcranial delivery of 980-nm CW laser pulses at a peak power of 2.0 W (25-ms pulses at 20 Hz over 1 s), an upconverted emission with a power density of ~0.063 mW/mm^2 was detected (Fig. 1H and fig. S5). This value was in line with our estimates based on the Kubelka-Munk theory when an empirical loss term was included (supplementary text). Further, considering that fiber photometry can only partially capture the emitted photons, this value represents a lower bound but nonetheless exceeds the level sufficient for ChR2 activation (fig. S6).

For the stimulation of a specific brain region, the power of transcranial NIR irradiation can be tuned according to its depth. NIR light is largely transparent, and its limited absorption results in minimal increases in local temperature because of constant circulation; thus, NIR pulses delivered across a wide range of laser energies to living tissue result in little photochemical or thermal damage (*27*, *28*). Nonetheless, at higher powers, it is important to consider a possible heating effect of NIR on the tissue. Our measurements of temperature change in the brain tissue showed that only mild temperature increases were induced under the conditions used in our study (supplementary text, figs. S7 and S8, and table S2). Immunohistochemical assessments further confirmed the absence of cytotoxicity (fig. S9). However, before a NIR strategy is adopted,

[1]Laboratory for Circuit and Behavioral Physiology, RIKEN Brain Science Institute, Wakoshi, Saitama 351-0198, Japan. [2]Department of Chemistry, National University of Singapore, Singapore 117543, Singapore. [3]Department of Neurophysiology, Graduate School of Medicine, The University of Tokyo, 7-3-1 Hongo, Bunkyo-ku, Tokyo 113-0033, Japan. [4]International Research Center for Neurointellegence (WPI), University of Tokyo Institute for Advanced Studies, The University of Tokyo, 7-3-1 Hongo, Bunkyo-ku, Tokyo 113-0033, Japan. [5]Department of Cellular Neurobiology, Graduate School of Medicine, The University of Tokyo, 7-3-1 Hongo, Bunkyo-ku, Tokyo 113-0033, Japan. [6]Singapore Institute for Neurotechnology (SINAPSE), National University of Singapore, Singapore 117456, Singapore. [7]Department of Biomedical Engineering, School of Medicine, Johns Hopkins University, Baltimore, MD 21205, USA. [8]Department of Neuropsychiatry, Keio University School of Medicine, Tokyo 160-8582, Japan. [9]Institute of Materials Research and Engineering, Agency for Science, Technology and Research, Singapore 117602, Singapore. [10]Department of Life Sciences, Graduate School of Arts and Sciences, The University of Tokyo, Tokyo, Japan.
*Corresponding author. Email: shuoshu@gmail.com (S.C.); chmlx@nus.edu.sg (X.L.); tjmchugh@brain.riken.jp (T.J.M.)

Downloaded from http://science.sciencemag.org/ on October 15, 2019

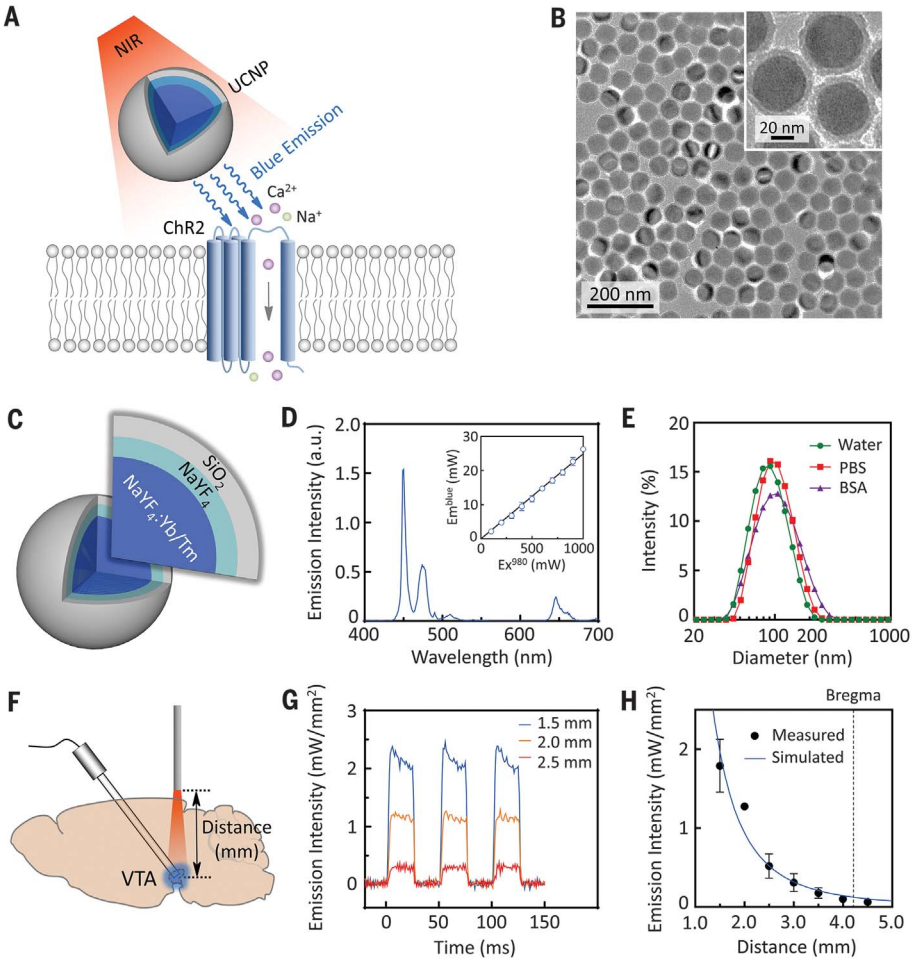

Fig. 1. UCNP-mediated NIR upconversion optogenetics for deep brain stimulation. (**A**) Schematic principle of UCNP-mediated NIR upconversion optogenetics. (**B**) Transmission electron microscopy (TEM) images of the silica-coated UCNPs. (Inset) High-resolution TEM image showing the core-shell structure. (**C**) Schematic design of a blue-emitting $NaYF_4$:Yb/Tm@SiO_2 particle. (**D**) Emission spectrum of the $NaYF_4$:Yb/Tm@SiO_2 particles under excitation at 980 nm. (Inset) Upconversion emission intensity of UCNPs [0.18 mg, 200 mg/ml in 900 nl of phosphate-buffered saline (PBS)] as a function of excitation intensity at 980 nm. (**E**) Size distribution of the UCNPs measured by dynamic light scattering. No aggregation is observed in water, PBS, or bovine serum albumin (BSA, 1 mg/ml in PBS) solution. (**F**) Scheme of in vivo fiber photometry for measuring UCNP-mediated NIR upconversion in deep brain tissue. The tip of an optic fiber transmitting NIR excitation light was positioned at various distances from the VTA where UCNPs were injected, and their emission was recorded by a second optic fiber. (**G**) Upconversion emission at the VTA upon 980-nm NIR irradiation (25-ms pulses at 20 Hz, 2.0-W peak power) from varying distances. (**H**) Measured (n = 4 mice) and simulated intensity of upconversion emission at the VTA as a function of the distance from the NIR irradiation source. Data are presented as mean ± SEM.

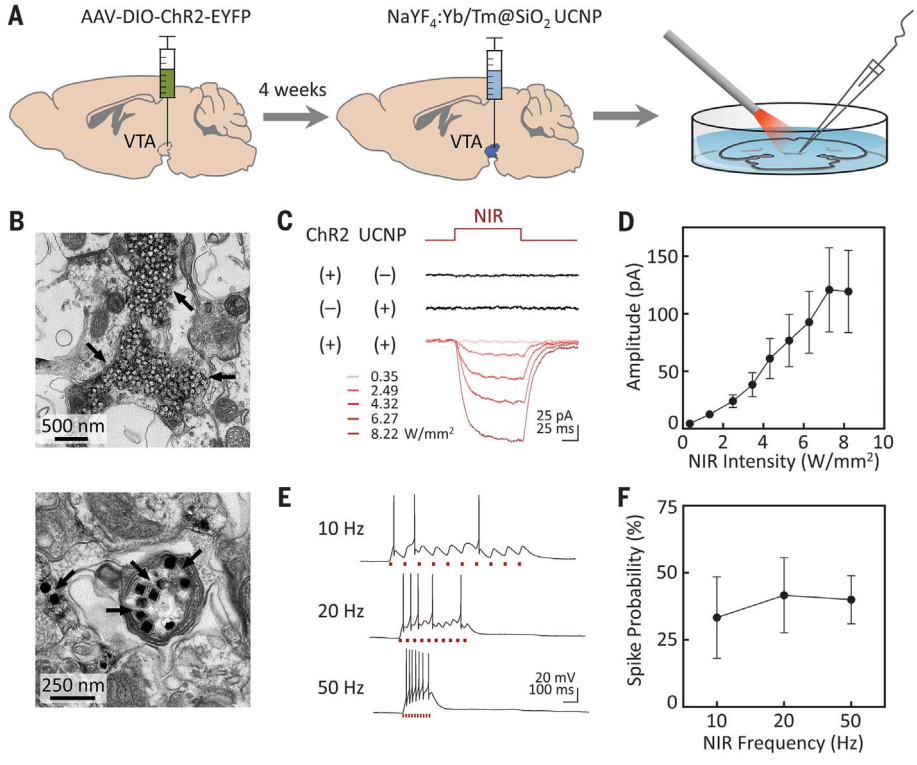

Fig. 2. NIR excitation of VTA DA neurons in vitro. (**A**) Experimental scheme. AAV-DIO-ChR2-EYFP was injected into the VTA of TH-Cre transgenic mice for Cre-dependent expression of ChR2 in DA neurons. Four weeks later, 900 nl of 200 mg/ml blue-emitting $NaYF_4$:Yb/Tm@SiO_2 UCNPs was injected into the VTA. Horizontal acute slices containing the VTA were prepared, and in vitro whole-cell recordings were performed. (**B**) Electron micrographs of UCNPs distributed in the VTA tissue. Black arrows indicate clusters of UCNPs. The upper image shows the distribution of the majority of UCNPs in extracellular space, and the lower image shows the uptake of UCNPs by an axon. (**C**) Voltage-clamp traces of neurons from VTA slice preparations in response to 100-ms NIR stimulation at various intensities. NIR light triggered photocurrents only in ChR2-transfected neurons in the presence of UCNPs. The traces for ChR2(−) and UCNP(−) controls in black were recorded under 8.22-W/mm^2 NIR irradiation. (**D**) Increase in photocurrent amplitude with elevated intensity of the NIR stimulation (n = 6 cells). (**E**) Current-clamp traces of a ChR2-expressing DA neuron in response to trains of 10 NIR pulses at different frequencies (20-ms pulses at 10 and 20 Hz, 10-ms pulses at 50 Hz, 8.22-W/mm^2 peak power) in the presence of UCNPs. Brief red lines indicate NIR pulses. (**F**) Spike probability as a function of the frequency of NIR stimulation (n = 6 cells). Data are presented as mean ± SEM.

Downloaded from http://science.sciencemag.org/ on October 15, 2019

the stimulation parameters should always be optimized for a balance between safety and efficacy.

To optimize the biocompatibility and long-term utility of UCNPs, we decorated the core-shell $NaYF_4$:Yb/Tm nanocrystals with silica ($NaYF_4$:Yb/Tm@SiO2) or poly(acrylic acid) (PAA) ($NaYF_4$:Yb/Tm@PAA). Both coating strategies resulted in monodispersed UCNPs of ~90-nm diameter (Fig. 1, B and E, and figs. S1 and S2) with similar luminescence profiles (Fig. 1D and fig. S1). One month after injection, UCNPs could still be observed at the target site, regardless of the type of coating (figs. S10 and S11), suggesting their long-term stability and low dispersion in tissue. We selected silica-coated UCNPs for in vivo upconversion optogenetics because they showed minimum cytotoxicity compared to the PAA-grafted ones, as indicated by less glial activation and lower macrophage accumulation in the VTA over prolonged exposure (figs. S10 and S11). This is likely a result of the silica coating that chemically stabilizes the nanoparticles and prevents direct contact of their lanthanide-doped core to cells within the tissue (*29*).

We chose the VTA for an initial examination of NIR stimulation because it is a deep brain region with a well-characterized anatomy and function. An adeno-associated virus (AAV) encoding ChR2-EYFP (enhanced yellow fluorescent protein) in a double-floxed inverted open reading frame (DIO) was injected into the VTA of tyrosine hydroxylase (TH)–driven Cre recombinase (TH-Cre) transgenic mice, resulting in Cre-dependent expression of ChR2 in dopamine (DA) neurons (Fig. 2A). Four weeks later, 900 nl of 200 mg/ml blue-emitting $NaYF_4$:Yb/Tm@SiO_2 UCNPs was injected into the VTA. We first assayed UCNP-mediated optogenetic activation of DA neurons in acute slices. Electron microscopy (Fig. 2B and fig. S12) showed that the UCNPs were localized in the injection area without extensive diffusion. The majority were distributed in extracellular spaces in the vicinity of cell membrane and synaptic clefts. A small fraction of UCNPs were taken up by neurons, mainly localized to axons, as well as by microglia. The confinement of UCNPs in the target brain region agrees with our light microscopy results showing that UCNPs exhibited minimal dispersion 1 month after injection (figs. S10 and S11). The 980-nm NIR pulses triggered membrane depolarization sufficient to generate photocurrents and evoke spikes in VTA DA neurons. The photocurrent amplitudes of ChR2 increased in response to elevated intensity of the incident NIR light under voltage clamp (Fig. 2, C and D). In the absence of UCNPs, no inward photocurrent was detected upon NIR irradiation (Fig. 2C). The activation kinetics of ChR2 by NIR upconversion was slower than that of blue light-activated ChR2 (fig. S6) (*30*) but comparable to that of recently reported red-shifted rhodopsins (*10*). NIR irradiation could also evoke action potentials of DA neurons, as shown in current-clamp traces. Trains of NIR illumination at 10 to 50 Hz elicited multiple spikes (Fig. 2E). The spike probability showed no significant dependence on the frequency of the NIR light (Fig. 2F).

We next tested the in vivo utility of UCNP-mediated NIR upconversion optogenetics. We sensitized VTA DA neurons of TH-Cre mice to transcranial NIR stimulation through viral delivery of ChR2 followed by bilateral UCNP injection (Fig. 3A). Anesthetized mice were exposed to transcranial pulsed NIR irradiation (15-ms pulses at 20 Hz, 3 s every 3 min for 30 min, 3.0-W peak power, 15-mW average power) delivered from an optical fiber (200 μm in diameter) placed 2 mm above the skull (1.4-W/mm^2 NIR on the skull surface). NIR-activated DA neurons

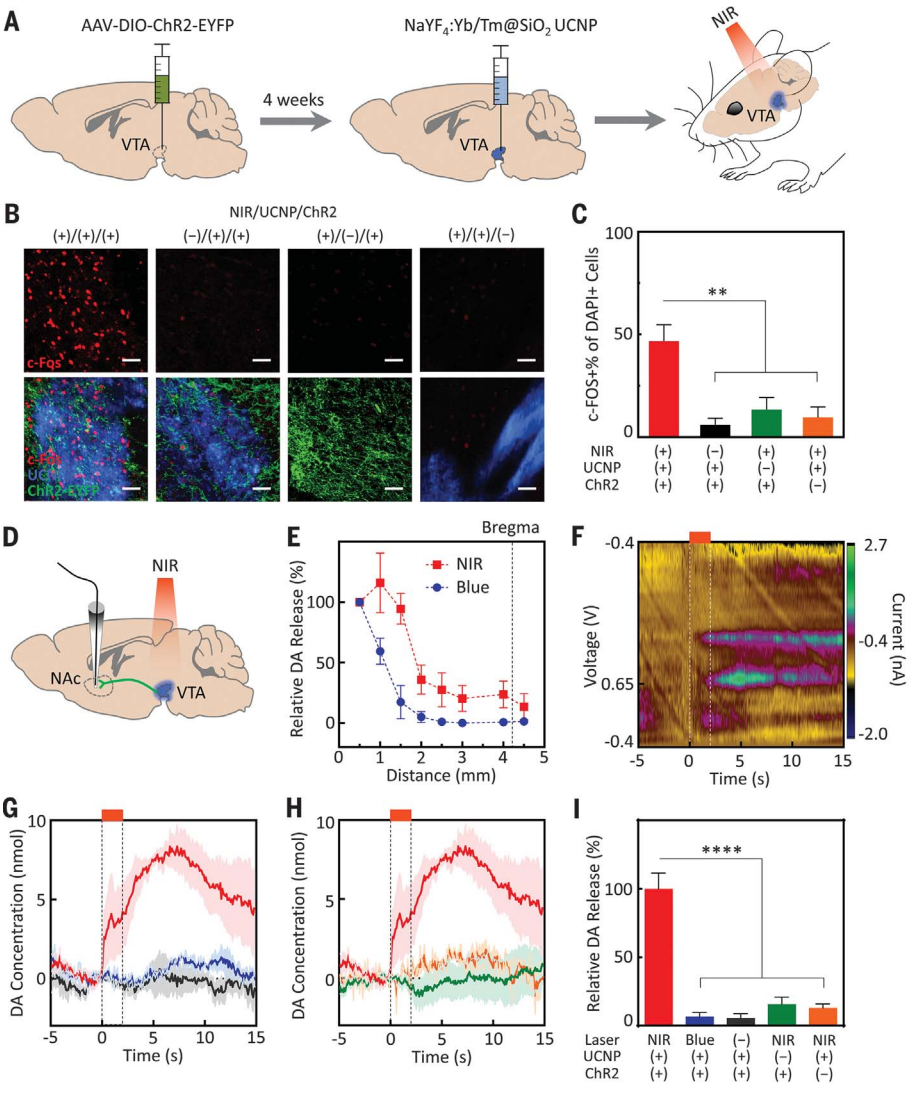

Fig. 3. Transcranial NIR stimulation of VTA DA neurons in vivo. (**A**) In vivo experimental scheme for transcranial NIR stimulation of the VTA in anesthetized mice. (**B**) Confocal images of the VTA after transcranial NIR stimulation under different conditions. Extensive NIR-driven c-Fos (red) expression was observed only in the presence of both UCNPs (blue) and ChR2 expression (labeled with EYFP, green). Scale bars: 100 μm. (**C**) Percentage of c-Fos–positive neurons within cell population indicated by DAPI (4′,6-diamidino-2-phenylindole), corresponding to the four conditions presented in (B) (n = 3 mice each, $F_{3,8}$ = 10.40, P < 0.01). (**D**) Scheme of in vivo FSCV to measure DA transients in ventral striatum during NIR stimulation of the VTA. (**E**) Relative DA signals in ventral striatum under NIR and blue-light stimulation of the VTA as a function of the distance from the light source to the VTA target. (**F**) A trace of background-subtracted current measured by FSCV in the ventral striatum of a nomifensine-pretreated mouse in response to transcranial NIR stimulation of the VTA (15-ms pulses at 20 Hz, 700-mW peak power). Vertical dashed lines marked by a horizontal orange line in between indicate the start and end of 2-s transcranial NIR stimulation. (**G** and **H**) Transient DA concentrations in ventral striatum in response to transcranial VTA stimulation under different conditions. Each color corresponds to a condition shown in (I). Significant DA release temporally locked to NIR stimulation was detected only in the presence of both UCNPs and ChR2 expression. (**I**) Cumulative DA release within 15 s after the start of transcranial stimulation under the five conditions presented in (G) and (H) ($F_{4,10}$ = 32.93, P < 0.0001). Data are presented as mean ± SEM.

Downloaded from http://science.sciencemag.org/ on October 15, 2019

were mapped by imaging the expression of c-Fos (Fig. 3, B and C, and fig. S13). Neuronal excitation was only triggered by NIR light in ChR2-transfected mice in the presence of UCNPs, as indicated by the significantly higher proportion of c-Fos–positive cells in areas where UCNP injection and ChR2 expression overlapped. We injected UCNPs to just one side of the VTA and observed NIR-induced c-Fos expression only in the injected hemisphere (fig. S14). We also observed up-regulation of c-Fos expression in the ventral striatum (fig. S15), which receives inputs from VTA DA neurons (*31*), indicating NIR-evoked excitation of postsynaptic structures of the targeted neurons. Control mice with UCNP injection, ChR2 expression, or NIR stimulation alone showed no significant c-Fos expression in either VTA or ventral striatum.

We evaluated the real-time efficacy of NIR-evoked excitation of VTA DA neurons with fast-scan cyclic voltammetry (FSCV) (Fig. 3D). Striatal DA transients reflect the phasic spike activity of VTA DA neurons (*31*) and have therapeutic implications for the treatment of major depression. In nomifensine-pretreated mice with both UCNP injection and ChR2 expression in VTA, we detected DA release that was temporally locked to transcranial NIR stimulation (15-ms pulses at 20 Hz, 700-mW peak power) (Fig. 3F). After a 2-s NIR stimulation, striatal DA release lasted for more than 15 s and peaked at ~5 s after light onset (Fig. 3, F and G). We detected no significant DA release in control mice with omission of NIR stimulation, UCNP injection, or ChR2 expression (Fig. 3, G to I). We compared the efficacy of NIR with blue light in evoking DA release by VTA DA neurons (Fig. 3E). The tip of an optic fiber transmitting NIR or blue light was positioned at various distances from the VTA target for optogenetic activation of DA neurons. When illuminating from a distance of 0.5 mm, NIR and blue light triggered similar amounts of DA release in ventral striatum (Fig. 3E and fig. S16). However, transcranial application of blue light did not result in striatal DA release (Fig. 3, E and I). Furthermore, NIR stimulation showed significantly slower attenuation in DA release with the increase of the distance from fiber tip to VTA (Fig. 3E).

We next expanded the application of in vivo upconversion optogenetics to multiple modes of neural control, including inhibition, as well as to different brain regions. First, we developed green-emitting UCNPs to match the maximum absorption of rhodopsins that hyperpolarize neurons, such as NpHR and Arch, to achieve non-invasive neuronal inhibition. The emission of UCNPs was tuned to ~540 nm by codoping Er^{3+} and Yb^{3+} into the $NaYF_4$ host lattice (Fig. 4A and fig. S1). We then assayed the ability of $NaYF_4$:Yb/Er@SiO_2 UCNPs to inhibit hippocampal activity during chemically induced hyperexcitability. Arch was virally expressed in excitatory neurons in the CA1 and dentate gyrus (DG) regions of the calcium-calmodulin–dependent kinase II (CamKII)–Cre mice, and green-emitting UCNPs were injected into the same region (Fig. 4B). Mice were

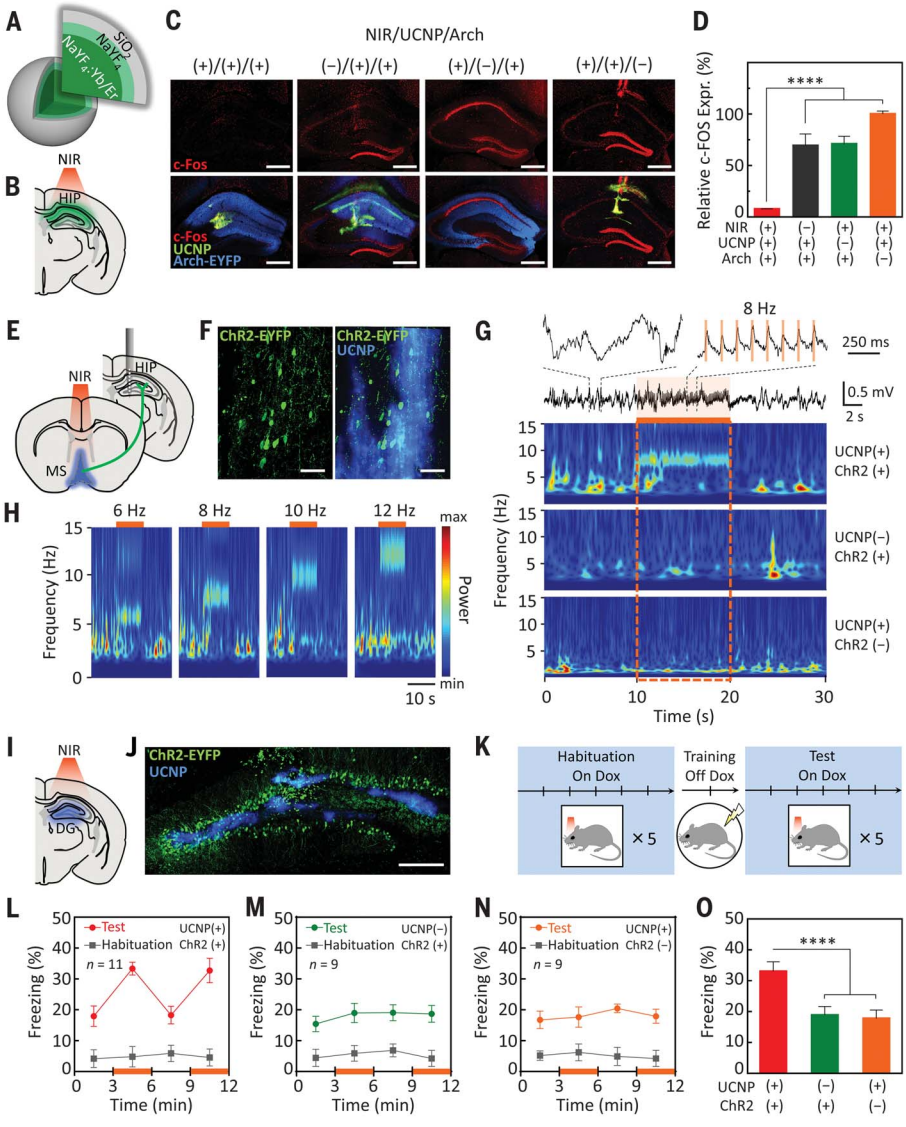

Fig. 4. Expanding in vivo upconversion optogenetics to multiple neural systems. (**A**) Schematic of a green-emitting $NaYF_4$:Yb/Er@SiO_2 particle. (**B**) Illustration of transcranial NIR inhibition of hippocampal (HIP) activity during chemically induced seizure. (**C**) Confocal images of the hippocampus following transcranial NIR stimulation under different conditions. Significant decrease in c-Fos (red) expression was observed only in the presence of both UCNPs (green) and Arch expression (labeled with EYFP, blue). Scale bars: 400 μm. (**D**) c-Fos expression under the four conditions presented in (C) (n = 3 mice each, $F_{3,8}$ = 94.02, P < 0.0001). (**E**) Illustration of transcranial NIR stimulation of medial septum (MS) for generation of theta oscillations. (**F**) Confocal images showing the overlap between ChR2-expressing PV interneurons (labeled by EYFP, green) and UCNPs (blue) in the MS of a PV-Cre mouse. Scale bars: 50 μm. (**G**) Hippocampal LFP in response to 8-Hz transcranial NIR stimulation (15-ms pulses, 10 s, 3.0-W peak power, 360-mW average power) of MS under different conditions. Top: Raw LFP trace from mouse with both UCNP and ChR2 injection. Bottom: Z-scored power in the theta range averaged across 30-s trials in all three conditions. (**H**) Transcranial NIR entrainment of hippocampal theta in a frequency-dependent manner. (**I**) Illustration of transcranial NIR stimulation of hippocampal engram for memory recall. (**J**) Confocal image showing the overlap between UCNPs (blue) and ChR2 expression (labeled with EYFP, green) in the DG of a mouse that underwent habituation, fear conditioning, and test sessions presented in (K). Scale bar: 200 μm. (**K**) Mice were on Dox food and habituated with NIR stimulation (15-ms pulses at 20 Hz, 250-mW peak power) in context A for 5 days, then off Dox food for 2 days and fear conditioned in context B. Mice were put back on Dox food and tested for 5 days in context A with transcranial NIR stimulation. (**L** to **N**) After fear conditioning, only c-fos-tTA mice with both ChR2 expression and UCNP injection showed increased freezing during 3-min NIR-on periods. Orange lines indicate the NIR-on epochs. (**O**) Summary of freezing levels of the three groups during test NIR-on epochs ($F_{2,26}$ = 105.9, P < 0.0001). Data are presented as mean ± SEM.

Downloaded from http://science.sciencemag.org/ on October 15, 2019

anesthetized and received the excitotoxin kainic acid (KA) at a dose used to induce seizure. We then applied transcranial low-intensity chronic pulsed NIR irradiation (3-ms pulses at 10 Hz, 120 min, 750-mW peak power, 22.5-mW average power) to inhibit neural activity in the hippocampus. Compared to all controls, mice with Arch expression, UCNP injection, and NIR stimulation showed a significant decrease in KA-induced c-Fos expression in the granule cells of the DG (Fig. 4, C and D), indicating effective silencing of hippocampal neurons by UCNP-mediated Arch activation. When NIR irradiation or Arch delivery was only unilaterally applied, distinct levels of c-Fos expression were observed between the two hemispheres (fig. S17).

Next, we examined if UCNP-mediated optogenetics could be used for noninvasive synchronization of neural activity. We targeted our NIR stimulation to inhibitory neurons in the medial septum, a key node in the network generating the theta oscillation (*32*, *33*). In vivo recordings of hippocampal local field potential (LFP) were performed during transcranial NIR irradiation of anesthetized parvalbumin (PV)–Cre mice with ChR2 expression and UCNP injection targeted to the medial septum (Fig. 4, E and F). Pulsed NIR stimulation in the theta frequency range (6 to 12 Hz) entrained the hippocampal theta oscillation in a frequency-dependent manner (Fig. 4, G and H). Control animals without ChR2 expression or UCNP injection showed no oscillation entrainment upon NIR irradiation (Fig. 4G).

Finally, we used the UCNP-mediated optogenetics to alter behavior of an awake animal by targeting NIR excitation to granule cells in the hippocampus involved in memory recall. Recent studies have demonstrated the neuronal activity–dependent tagging of memory-encoding hippocampal neurons by ChR2 and subsequent optogenetic reactivation of these engrams (*34*). We injected blue-emitting UCNPs into the DG of c-fos-tTA (tetracycline transcriptional activator) transgenic mice and labeled active c-Fos–expressing DG granule cells with ChR2 during the encoding of fear memory in the absence of doxycycline (Dox) (Fig. 4, I to K, and fig. S18). We then applied transcranial NIR stimulation (15-ms pulses at 20 Hz, 250-mW peak power) to reactivate labeled granule cells. NIR irradiation increased freezing behavior of the mice during laser illumination in a safe context (Fig. 4L). Animals with no UCNP injection or ChR2 expression showed no significant change in freezing when NIR irradiation was applied (Fig. 4, M to O). Moreover, the behavioral effect of NIR stimulation in this experiment was observed 2 weeks after the injection of UCNPs, indicating their long-term in vivo utility. This timing is consistent with our findings that no extensive diffusion or degradation of UCNPs was observed 1 month after injection (figs. S10 and S11).

These findings demonstrate that UCNP-mediated optogenetics is a flexible and robust minimally invasive nanotechnology-assisted approach for optical control of in vitro and in vivo neuronal activity. We show spectral tuning of UCNPs for compatibility with the current toolbox of light-activated channels (*9*) that is sufficient for functional activation and inhibition across a variety of deep brain structures. Future characterization of the interaction of UCNPs with neural tissue will allow for better biocompatibility and long-term utility. In parallel, systematic optimization of the dose of UCNP injection and the parameters of NIR stimulation will provide improved accuracy and safety. Such data might also present an upper limit to the adaptability and efficiency of NIR stimulation. Furthermore, refinements of the nanoparticles to establish precise cell-type or intracellular targeting (*17*, *18*), as well as improved delivery methods that would further reduce invasiveness (*35*), will advance the utility of the approach. These methods, combined with the enhanced ability to express light-sensitive channels in the brain, may allow UCNP-mediated neuronal control to complement or extend current approaches to deep brain stimulation and neurological disorder therapies.

REFERENCES AND NOTES

1. A. M. Lozano, N. Lipsman, *Neuron* **77**, 406–424 (2013).
2. E. Dayan, N. Censor, E. R. Buch, M. Sandrini, L. G. Cohen, *Nat. Neurosci.* **16**, 838–844 (2013).
3. N. Grossman *et al.*, *Cell* **169**, 1029–1041.e16 (2017).
4. R. Chen, G. Romero, M. G. Christiansen, A. Mohr, P. Anikeeva, *Science* **347**, 1477–1480 (2015).
5. S. A. Stanley *et al.*, *Nature* **531**, 647–650 (2016).
6. W. Legon *et al.*, *Nat. Neurosci.* **17**, 322–329 (2014).
7. R. Airan, *Science* **357**, 465 (2017).
8. M. R. Hamblin, *BBA Clin.* **6**, 113–124 (2016).
9. L. Fenno, O. Yizhar, K. Deisseroth, *Annu. Rev. Neurosci.* **34**, 389–412 (2011).
10. J. Y. Lin, P. M. Knutsen, A. Muller, D. Kleinfeld, R. Y. Tsien, *Nat. Neurosci.* **16**, 1499–1508 (2013).
11. F. Zhang *et al.*, *Nat. Neurosci.* **11**, 631–633 (2008).
12. O. Yizhar *et al.*, *Nature* **477**, 171–178 (2011).
13. A. S. Chuong *et al.*, *Nat. Neurosci.* **17**, 1123–1129 (2014).
14. N. C. Klapoetke *et al.*, *Nat. Methods* **11**, 338–346 (2014).
15. P. Rajasethupathy *et al.*, *Nature* **526**, 653–659 (2015).
16. R. Prakash *et al.*, *Nat. Methods* **9**, 1171–1179 (2012).
17. G. Chen, H. Qiu, P. N. Prasad, X. Chen, *Chem. Rev.* **114**, 5161–5214 (2014).
18. B.Zhou, B. Shi, D. Jin, X. Liu, *Nat. Nanotechnol.* **10**, 924–936 (2015).
19. K. A. Deisseroth, P. Anikeeva, Upconversion of light for use in optogenetic methods. United States Patent PCT/US2011/059287 (2011).
20. S. Hososhima *et al.*, *Sci. Rep.* **5**, 16533 (2015).
21. S. Shah *et al.*, *Nanoscale* **7**, 16571–16577 (2015).
22. X. Wu *et al.*, *ACS Nano* **10**, 1060–1066 (2016).
23. A. Bansal, H. Liu, M. K. Jayakumar, S. Andersson-Engels, Y. Zhang, *Small* **12**, 1732–1743 (2016).
24. X. Ai *et al.*, *Angew. Chem. Int. Ed. Engl.* **56**, 3031–3035 (2017).
25. T. Vo-Dinh, Ed., *Biomedical Photonics Handbook* (CRC Press, Boca Raton, FL, 2003).
26. L. A. Gunaydin *et al.*, *Cell* **157**, 1535–1551 (2014).
27. A. Bozkurt, B. Onaral, *Biomed. Eng. Online* **3**, 9 (2004).
28. T. A. Henderson, L. D. Morries, *Neuropsychiatr. Dis. Treat.* **11**, 2191–2208 (2015).
29. J. N. Liu, W. B. Bu, J. L. Shi, *Acc. Chem. Res.* **48**, 1797–1805 (2015).
30. E. S. Boyden, F. Zhang, E. Bamberg, G. Nagel, K. Deisseroth, *Nat. Neurosci.* **8**, 1263–1268 (2005).
31. M. J. Wanat, I. Willuhn, J. J. Clark, P. E. Phillips, *Curr. Drug Abuse Rev.* **2**, 195–213 (2009).
32. R. Boyce, S. D. Glasgow, S. Williams, A. Adamantidis, *Science* **352**, 812–816 (2016).
33. L. L. Colgin, *Annu. Rev. Neurosci.* **36**, 295–312 (2013).
34. X. Liu *et al.*, *Nature* **484**, 381–385 (2012).
35. D. Ni *et al.*, *ACS Nano* **8**, 1231–1242 (2014).

ACKNOWLEDGMENTS

We thank S. Wada and T. Tsukihana (RIKEN Center for Advanced Photonics) for technical advice and assistance with laser optics; H. Hirase [RIKEN Brain Science Institute (BSI)] for helpful discussion on in vivo toxicity assay and gifts of antibodies against GFAP (glial fibrillary acidic protein) and Iba1; S. Itohara (RIKEN BSI) for the gift of antibody against Caspase-3; T. Launey (RIKEN BSI) for helpful discussion on electron microscopy; and C. Yokoyama (RIKEN BSI) and F. Xu (University of Science and Technology of China) for comments on the manuscript. This work was supported by JSPS (Japan Society for the Promotion of Science) Postdoctoral Fellowship (16F16386) (S.C.); RIKEN Special Postdoctoral Researchers Program (S.C.); RIKEN BSI (T.J.M.); Grant-in-Aid for Scientific Research on Innovative Areas from MEXT (the Ministry of Education, Culture, Sports, Science and Technology of Japan) (17H05591) (T.J.M.); Grant-in-Aid for Young Scientists B (16K18373) (S.C.); the Singapore Ministry of Education (grant R143000627112, R143000642112) (X.L.); the National Research Foundation of Singapore under its Competitive Research Programme (CRP Award no. NRF-CRP15-2015-03) (X.L.); Grants-in-Aid for Scientific Research (25000015) (M.K.); Grants-in-Aid for Scientific Research (17H01387 and 25117006) (S.O.); and Core Research for Evolutional Science and Technology from the Japanese Science and Technology Agency (JPMJCR14W2) (S.O.). All data necessary to assess the conclusions of this research are available in the text and supplementary materials. Data related to the synthesis and characterization of UCNPs are available via the X.L. laboratory website (http://liuxg.science.nus.edu.sg). Data related to the application of UCNP-mediated optogenetics in the mouse brain are archived on the servers of Laboratory for Circuit and Behavioral Physiology at the RIKEN Brain Science Institute and accessible at http://cbp.brain.riken.jp/chen_et_al. All materials are available upon request.

SUPPLEMENTARY MATERIALS

www.sciencemag.org/content/359/6376/679/suppl/DC1
Materials and Methods
Supplementary Text
Figs. S1 to S18
Tables S1 and S2
References (*36*–*46*)

3 October 2017; accepted 7 December 2017
10.1126/science.aaq1144

Downloaded from http://science.sciencemag.org/ on October 15, 2019

Science

Near-infrared deep brain stimulation via upconversion nanoparticle–mediated optogenetics

Shuo Chen, Adam Z. Weitemier, Xiao Zeng, Linmeng He, Xiyu Wang, Yanqiu Tao, Arthur J. Y. Huang, Yuki Hashimotodani, Masanobu Kano, Hirohide Iwasaki, Laxmi Kumar Parajuli, Shigeo Okabe, Daniel B. Loong Teh, Angelo H. All, Iku Tsutsui-Kimura, Kenji F. Tanaka, Xiaogang Liu and Thomas J. McHugh

Science **359** (6376), 679-684.
DOI: 10.1126/science.aaq1144

Stimulating deep inside the brain

Noninvasive deep brain stimulation is an important goal in neuroscience and neuroengineering. Optogenetics normally requires the use of a blue laser inserted into the brain. Chen *et al.* used specialized nanoparticles that can upconvert near-infrared light from outside the brain into the local emission of blue light (see the Perspective by Feliu *et al.*). They injected these nanoparticles into the ventral tegmental area of the mouse brain and activated channelrhodopsin expressed in dopaminergic neurons with near-infrared light generated outside the skull at a distance of several millimeters. This technique allowed distant near-infrared light to evoke fast increases in dopamine release. The method was also used successfully to evoke fear memories in the dentate gyrus during fear conditioning.

Science, this issue p. 679; see also p. 633

ARTICLE TOOLS http://science.sciencemag.org/content/359/6376/679

SUPPLEMENTARY MATERIALS http://science.sciencemag.org/content/suppl/2018/02/07/359.6376.679.DC1

RELATED CONTENT http://science.sciencemag.org/content/sci/359/6376/633.full

REFERENCES This article cites 44 articles, 4 of which you can access for free
http://science.sciencemag.org/content/359/6376/679#BIBL

PERMISSIONS http://www.sciencemag.org/help/reprints-and-permissions

Use of this article is subject to the Terms of Service

Science (print ISSN 0036-8075; online ISSN 1095-9203) is published by the American Association for the Advancement of Science, 1200 New York Avenue NW, Washington, DC 20005. The title *Science* is a registered trademark of AAAS.

Copyright © 2018 The Authors, some rights reserved; exclusive licensee American Association for the Advancement of Science. No claim to original U.S. Government Works

Downloaded from http://science.sciencemag.org/ on October 15, 2019